

Proceedings of the 20th INSECT 2024

International Symposium on ElectroChemical Machining Technology 2024

Aachen, November 18-19, 2024

Thomas Bergs, Elio Tchoupe Sambou, Timm Petersen,
Tim Herrig, Andreas Klink (Eds.)

Manufacturing Technology Institute – MTI
RWTH Aachen University

Imprint

Proceedings of the 20th INSECT 2024

International Symposium on Electrochemical Machining Technology 2024

Aachen, November 18-19, 2024

Editors

Thomas Bergs

Elio Tchoupe Sambou

Timm Petersen

Tim Herrig

Andreas Klink

Manufacturing Technology Institute – MTI, RWTH Aachen University

Campus-Boulevard 30

52074 Aachen

Available via the institutional repository of RWTH Aachen University:

DOI: 10.18154/RWTH-2024-10228

Aachen 2024

This work is licensed under a

Creative Commons Attribution 4.0 International license.

Excluded from this license are photos in which persons are recognizably depicted and all logos shown.

Study of Pulse Electrochemical Machining on Conventionally and Additively Manufactured Inconel 718 Workpieces

A. Frank[a], T. Hall[a,b], M. Zeiner[a,b], D. Bähre[a,b]*

[a]Center for Mechatronics and Automation Technology (ZeMA gGmbH), Gewerbepark Eschberger Weg 46, Gebäude 9, 66121 Saarbrücken, Germany

[b]Institute of Production Engineering, Saarland University, Campus A4.2, 66123 Saarbrücken, Germany

*Corresponding author: alexander.frank@zema.de

DOI: 10.18154/RWTH-2024-10230

Abstract

Due to their exceptional mechanical properties, high-temperature resistant materials such as Inconel 718 are widely used in the construction of aircraft and turbines. These applications necessitate both, high precision manufactured components and exceedingly complex component shapes. Conventional manufacturing processes face limitations when working with these materials due to their high hardness and strength. Metal additive manufacturing offers a promising solution, providing significant design freedom. However, for applications with distinctive fluid dynamics, the desired precision and the surface quality are not yet sufficient. Pulse Electrochemical Machining (PECM) is a high-precision post-processing method based on anodic metal dissolution, that is independent of the mechanical properties of the material. The aim of this study is to evaluate the suitability of the PECM process for post-processing additively manufactured Inconel 718 components. Therefore, the electrochemical dissolution behavior of the additively manufactured workpieces of this nickel-base superalloy is compared with that of conventionally manufactured counterparts.

1 Introduction

The nickel-base superalloy Inconel 718 (IN718) is well-known for its exceptional mechanical properties, which ensure high strength at high temperatures up to

700 °C in combination with very good corrosion and oxidation resistance [1]. Consequently, IN718 is widely employed in the construction of aircraft engine components, specifically turbine blades and blisks. Conversely, these properties present challenges to the machining of Inconel using conventional methods, particularly in the production of precise geometries and high-quality surfaces [2].

Additive manufacturing processes, such as Laser-Powder Bed Fusion (L-PBF), enable the construction of near-net-shape components with complex geometries utilizing powder-based materials, thereby minimizing the remaining volume to be removed [3]. However, the desired precision and the surface quality are not yet sufficient for applications with specific demands regarding flow properties. Thus, a finishing method is necessary that is also compatible with hard-to-machine materials, such as IN718.

Pulse electrochemical machining (PECM) as post-processing method could offer an alternative process route, as it enables non-contact surface processing, independent of the mechanical properties of the workpiece and without thermal energy input [4] resulting in very high surface qualities. Previous studies by Herter et al. [5] and Schröder et al. [6] have demonstrated the suitability of electrochemical machining technology for post-processing additively manufactured stainless steel and aluminum components. Furthermore, the machining of support structures on additively manufactured components is also feasible with the PECM process, as demonstrated by the findings of Hall et al. [7] and Zeiner et al. [8]. In the case of the IN718 alloy, Wang et al. [9] and Guo et al. [10] showed that electrochemical machining (ECM) is suitable for additively manufactured parts. L-PBF manufactured IN718 parts were previously machined electrochemically by Jain et al. [11] and Herter et al. [12] resulting in satisfactory surface quality. Zhu et al. [13] demonstrated that the reachable surface quality is very dependent on the microstructure of the IN718 machined with ECM, as the matrix is dissolved more strongly than the niobium-rich phases within the microstructure. As additive manufacturing leads to significantly different microstructures, comprehensive investigations under comparable conditions are necessary regarding the electrochemical dissolution behavior.

In this work, the suitability of the PECM process for post-processing additively manufactured Inconel 718 components is evaluated. Therefore, the electrochemical dissolution behavior of the additively manufactured workpieces of the nickel-base superalloy is compared with that of conventionally manufactured counterparts.

2 Materials and experimental setup

As the anode material (workpiece), samples of the Inconel 718 alloy (NiCr19NbMo) were produced in two groups. The first set of samples was manufactured conventionally by means of Vacuum Induction Melting followed by annealing and turning to create cylindrical rods with a diameter of 10 mm and a height of 50 mm. The second set of cylindrical rods was produced additively using the L-PBF technology, whereby the workpieces are built up layer-by-layer using laser light to selectively melt the metal powder in the powder bed. Energy Dispersive X-ray Spectroscopy (EDS) measurements confirmed that the chemical composition of the different sample groups was identical.

The electrochemical processing was performed in the form of frontal gap experiments on the industrial PECM-machine *PEMCenter8000* by *PEMTec SNC (Forbach, France)*, using $NaNO_3$-based electrolyte. The cathode (tool) is made of stainless steel 1.4301 and 12 mm wide in diameter. Lateral electrolyte flushing between the electrodes is realized by using an additively manufactured flushing chamber made of *Formlaps Clear Resin*, and thus ensures equal flushing conditions during the experiments. The process parameters are given in Table 1.

Table 1: *PECM process parameters.*

Variable process parameter	***Manufacturing type***	***Levels***					
Feed rate v_f [mm/min]	*Conventionally & Additively (L-PBF)*	*0.08*	*0.10*	*0.13*	*0.15*	*0.17*	*0.20*
		0.25	*0.27*	*0.30*	*0.33*	*0.36*	

Constant process parameters			
Process voltage [V]	*12*	*Electrolyte conductivity [mS/cm]*	*148 ± 5*
Pulse on-time [ms]	*5*	*Electrolyte temperature [°C]*	*31.5 ± 1.0*
Mech./Electr. frequency [Hz]	*50*	*Electrolyte pressure [kPa]*	*200*
Voltage pulse duty cycle [%]	*50*	*pH-value*	*8.0 ± 0.2*

The parameters were determined in preliminary tests and kept constant for all samples. To investigate the electrochemical dissolution behavior of the two manufacturing types, only the feed rate is varied in the specified levels. Each level of the feed rate is repeated three times in the same procedure for statistical validation. A total of 66 tests are performed. For the determination of the

Specific Mass Removal value (SMR), the mass of the samples is measured before and after each test run using a precision scale *K-M SRK-100* by *Krahl-Messtechnik (Bovenden, Germany)* with a precision of d = 0.001 g. To keep the measurement error below 1%, at least 0,5 mm of the anode was removed in each test. The surface evaluation is carried out optically with the scanning electron microscope (SEM) *Zeiss Sigma VP* by *Carl Zeiss Microscopy GmbH (Jena, Germany)* and the digital microscope *Keyence VHX 7000* by *Keyence Corporation* (*Osaka, Japan*). Tactile evaluation was measured on a perthometer *MarSurf XR/XT20* by *Mahr (Göttingen, Germany)*.

3 Results and discussion

The results of PECM processing for conventional and additive manufactured parts are shown in the following graphs, which present the mean values of the three test series for each material type. Figure 1 illustrates the feed rate as a function of current density for both manufacturing types. The data exhibit linear proportionality and only very slight deviations, indicating a constant and equal reaction mechanism. It can be observed that the L-PBF parts exhibit lower current densities than the conventional parts at the same feed rates. This phenomenon can be attributed to the fact that the density measurements confirm a lower relative density of 99,75 % for the additive material. This is due to the presence of pores within the sample volume. The current density is influenced by the material density in a proportional manner. Machining at a feed rate of 0.36 mm/min and a current density of approximately 110 A/cm² for conventional and 93 A/cm² for L-PBF material turned out to be the upper limit for all specimens, since gap widths of 10 µm or less were reached, as depicted in Figure 2. As the gap width decreases, the process conditions become increasingly unstable, thereby increasing the risk of short circuits. In accordance with Faraday's law, the gap width is inversely proportion to the current density. As expected for the $NaNO_3$-electrolyte used, Figure 3 indicates, that the Specific Mass Removal (SMR) values align with the current density towards a plateau of approximately 0.19 mg/C. The deviating SMR value at highest current density is caused by processing at the limit of stable machining range.

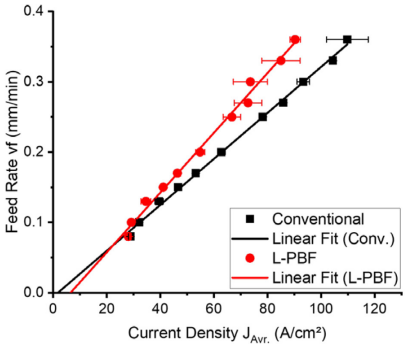

Figure 1: *Feed rate vs. current density.*

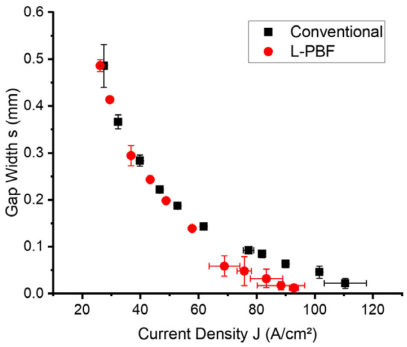

Figure 2: *Gap width vs. current density.*

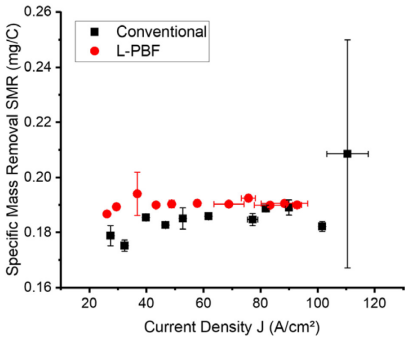

Figure 3: *SMR vs. current density.*

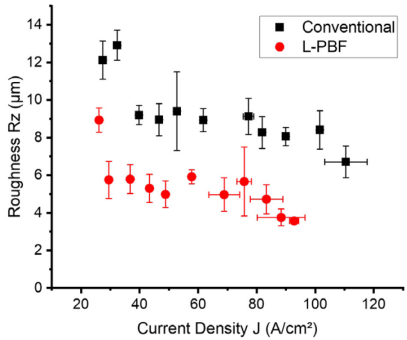

Figure 4: *Average roughness depth R_z vs. current density.*

The most significant contrasts are found upon examination of the resulting surfaces after processing. Figure 4 shows the results of the tactile measurements of the average roughness R_z, which continuously improves to smaller values for both types with increasing current densities. These values present the mean values of measurements taken along and across the flushing direction, to account for possible influences of flushing grooves. However, the L-PBF samples achieve significantly lower R_z values with the same process parameters, averaging 3.57 µm at the highest current density, while the conventional samples only achieve 6.71 µm. A similar trend is evident when examining the R_a values, which result in values of 0.59 µm and 0.96 µm respectively. Since both the chemical composition and the process conditions were identical, such differences must be due to the microstructural differences in roughness and achievable current densities of the sample types.

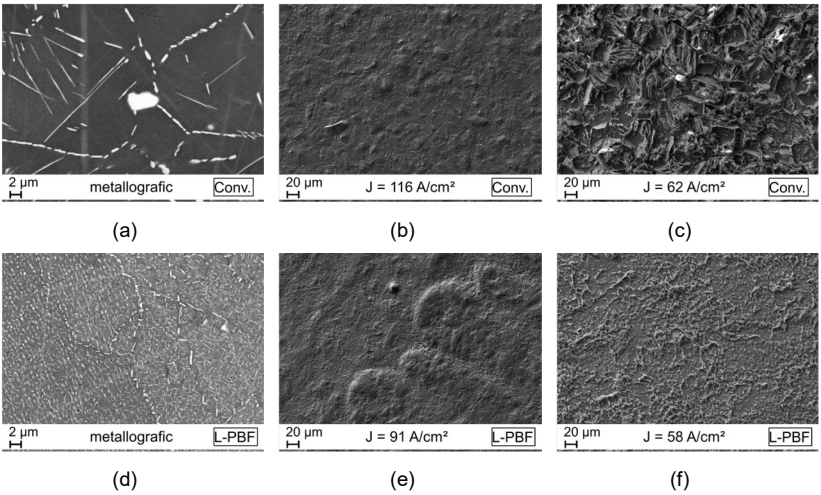

Figure 5: *SEM images for comparison of the conventionally and L-PBF manufactured workpieces respectively, showing (a,d) the microstructures of prior to PECM machining, (b,e) the highest surfaces qualities after PECM-machining at highest feed rate and current density and (c,f) the oxide layer formation at medium current densities.*

Accordingly visual evaluation was conducted. In order to evaluate the initial condition prior to electrochemical processing, one sample each was metallographically polished and analysed using SEM. Figure 5(a, d) show that the phases of the microstructure are significantly smaller as a consequence of the L-PBF manufacturing compared to the conventional material. The needle-shaped phases inside the grains are also significantly finer. This is also evident after PECM processing. In Figure 5(b), the grains, grain boundary phases and carbides or nitrides are clearly visible on the surface, due to the selective dissolution of the microstructure. The found protrusion of grains of the microstructure from the sample surface by several microns is responsible for the observed roughness values. In comparison, the surface of L-PBF manufactured parts in Figure 5(e) is much smoother, due to the finer microstructure, when topographic influences from the laser scan tracks are disregarded. Those scan tracks and patterns originate from the additive manufacturing process and are found for all the additive samples after PECM machining. By utilizing depth-focused three-dimensional images obtained from the digital microscope, the height of 11 representative scan tracks was quantified, yielding an average height of approximately 4.15 µm. This value is consistent with the range of R_z values observed. It can be concluded that the topography of the scan tracks limits the achievable surface quality for the L-PBF parts. The results of the EDS measurements and

element mappings indicate that there is an accumulation of niobium and molybdenum at the edges of the scan tracks, with slightly higher numbers of these elements. These elements are more difficult to dissolve electrochemically, which could explain the elevation of these areas from the surface. After processing, most of the oxide surface layers that were loosely adhering to the surface of both sample types were removed by cleaning with water and cloth wiping. For the chemical analysis of these oxide layers, they were not removed for the samples in Figure 5(c, d). The EDS analyses demonstrate that the oxide layers haven an identical chemical composition for both manufacturing types and are primarily composed of nickel and niobium oxides. Furthermore, the analysis revealed the presence of intact niobium carbide and titanium nitride blocks embedded within the oxide layers. Nevertheless, a visual comparison indicates that the layer for the L-PBF samples is significantly thinner. Initial investigations have led to the hypothesis that this is also due to the microstructure. The element niobium is present in the significantly finer microstructure of the L-PBF parts in the grain boundary phases, as precipitates in the grain centre and in the form of niobium carbide blocks in the same quantity, but in smaller dimensions. During the formation of the oxide layer, these smaller niobium particles might therefore be better removed by the electrolyte flushing and form a thin oxide layer. This hypothesis requires further investigations.

4 Conclusion

In this study, the electrochemical dissolution behavior and machinability of IN718 parts manufactured by L-PBF and their conventionally manufactured counterparts were determined using an industrial PECM-production machine. Despite the machining conditions were kept identical, differences in the machinability and achievable surface quality were observed, which could be attributed to the differences in the microstructure. The additive parts exhibited lower current densities at identical feed rates, a consequence of the reduced material density resulting from the manufacturing process. However, a notable discrepancy in surface roughness was found. The surface roughness of the conventional samples is primarily influenced by the coarser microstructure. Conversely, the microstructure has less of an impact on the additive parts, which is due to the significantly finer microstructure resulting from the manufacturing process. It can be concluded that significantly lower roughness can be achieved for the L-PBF parts despite the higher initial roughness, which is only limited by the topographical appearance of the laser-induced scan tracks. Furthermore, a

less intense oxide layer formation was found for the additive parts, which is also attributes to the microstructure in the initial hypothesis. The favorable results for additively manufactured L-PBF parts prove the suitability of the PECM method for post-processing.

Acknowledgements

The authors thank the European Regional Development Fund (ERDF) for supporting their research within the project “VProSaar”.

Literature

[1] *Weißbach, W.: Werkstoffkunde. Strukturen, Eigenschaften, Prüfung. 16. Überarbeitete Auflage. Friedr. Vieweg & Sohn Verlag / GWV Fachverlage GmbH. Wiesbaden, 2007.*

[2] *Klocke, F.; Zeis, M.; Klink, A.; Veselovac, D.:Technological and economical comparison of roughing strategies via milling, EDM and ECM for titanium- and nickel-based blisks. In: Procedia CIRP. Volume 2, 2012, p. 98-101.*

[3] *Uhlmann, E.; Bergmann, A.; John, F.: Generative Herstellung von Implantaten. Neue Konzepte für Werkzeugmaschinen. Fraunhofer Gesellschaft. 6. Berliner Runde, 2011.*

[4] *Klocke, F.; König, W. Fertigungsverfahren 3 – Abtragen, Generieren und Lasermaterialbearbeitung. Book, 4. Edn., Springer Berlin, 2007.*

[5] *Herter, F.; Hall, T.; Bergmann, A.; Bähre, D.: Experimental comparison of electrochemical machining of selective laser melted and conventionally produced specimens. Proceedings of the 14th International Symposium on Electrochemical Machining Technology INSECT, Aachen, 2018, p. 17-24.*

[6] *Schröder, S.; Petzold, T.; Martin, A.; Schubert, A.: Pulsed electrochemical machining of 1.2709 additive manufactured steel. Proceedings of the 16th International Symposium on Electrochemical Machining Technology INSECT, Chemnitz, 2020, p. 85-92.*

[7] *Hall, T.; Herter, F.; Zeiner, M.; Bähre, D.: Experimental study on removing support structures of additively manufactured metal parts using pulse electrochemical machining. Proceedings of the 17th International*

Symposium on Electrochemical Machining Technology INSECT, Leuven, 2021, p. 177-184.

[8] Zeiner, M.; Hall, T.; Herter, F.; Bähre, D.: Pulsed electrochemical machining (PECM) of additively manufactured parts with focus on removing support structures. Proceedings of the 18th International Symposium on Electrochemical Machining Technology INSECT, Tokyo, 2022, p. 15-22.

[9] Wang, X.; Qu, N.; Guo, P.; Fang, X.; Lin, X.: Electrochemical Machining Properties of the Laser Rapid Formed Inconel 718 Alloy in NaNO3 Solution. Journal of the Electrochemical Society 164, 2017, p. E548-E559.

[10] Guo, P.; Lin, X.; Xu, J.; Li, J.; Liu, J.; Huang, W.: Electrochemical Removal of Different Phases from Laser Solid Formed Inconel 718. Journal of the Electrochemical Society 164, 2017, p. E151-E157.

[11] Jain, S.; Corliss, M.; Tai, B.; Nguyen Hung, W.: Electrochemical polishing of selective laser melted Inconel 718. Procedia Manufacturing 34, 2019, p. 239-246.

[12] Herter, F.; Ernst, A.; Bergmann, A.; Bähre, D.: Experimental study of electrochemical machining of selective laser melted Inconel 718. Proceedings of the 16th International Symposium on Electrochemical Machining Technology INSECT, Chemnitz, 2020, p. 71-76.

[13] Zhu, D.; Yu, L.; Zhang, R.: Dissolution Effects with Different Microstructures of Inconel 718 on Surface Integrity in Electrochemical Machining. Journal of the Electrochemical Society 165, 2018, p. E872-E878.